Synthetic and Systems Biotechnology 9 (2024) 445–452

Contents lists available at ScienceDirect

Synthetic and Systems Biotechnology

journal homepage: www.keaipublishing.com/en/journals/synthetic-and-systems-biotechnology

Original Research Article

# Analyzing and engineering of the biosynthetic pathway of mollemycin A for enhancing its production

Shixue Jin [a], Huixue Chen [a], Jun Zhang [b], Zhi Lin [b], Xudong Qu [b], Xinying Jia [c,d,**], Chun Lei [a,*]

[a] School of Pharmacy, Fudan University, Shanghai, 201203, China
[b] State Key Laboratory of Microbial Metabolism and School of Life Sciences and Biotechnology, Shanghai Jiao Tong University, Shanghai, 200240, China
[c] Australian Institute for Bioengineering and Nanotechnology, The University of Queensland, St Lucia, QLD, 4072, Australia
[d] Department of Biochemistry, National University of Singapore, 14 Medical Dr, Singapore, 117599

ARTICLE INFO

*Keywords:*
Mollemycin A
Gene cluster
Biosynthetic pathway
Biosynthetic engineering
Production enhancement
Azinothricin

ABSTRACT

Mollemycin A (MOMA) is a unique glyco-hexadepsipeptide-polyketide that was isolated from a *Streptomyces* sp. derived from the Australian marine environment. MOMA exhibits remarkable inhibitory activity against both drug-sensitive and multidrug-resistant malaria parasites. Optimizing MOMA through structural modifications or product enhancements is necessary for the development of effective analogues. However, modifying MOMA using chemical approaches is challenging, and the production titer of MOMA in the wild-type strain is low. This study identified and characterized the biosynthetic gene cluster of MOMA for the first time, proposed its complex biosynthetic pathway, and achieved an effective two-pronged enhancement of MOMA production. The fermentation medium was optimized to increase the yield of MOMA from 0.9 mg $L^{-1}$ to 1.3 mg $L^{-1}$, a 44% boost. Additionally, a synergistic mutant strain was developed by deleting the *momB3* gene and overexpressing *momB2*, resulting in a 2.6-fold increase from 1.3 mg $L^{-1}$ to 3.4 mg $L^{-1}$. These findings pave the way for investigating the biosynthetic mechanism of MOMA, creating opportunities to produce a wide range of MOMA analogues, and developing an efficient strain for the sustainable and economical production of MOMA and its analogues.

## 1. Introduction

Malaria, a life-threatening infectious disease caused by parasites of the genus *Plasmodium*, affected an estimated 249 million people globally in 2022, with 608,000 estimated deaths. [1]. A critical component in the fight against malaria is the effective treatment with potent drugs. The emergence of resistance to artemisinin and its partner drugs in *Plasmodium falciparum*, however poses a significant threat to global efforts to reduce the burden of malaria [2]. Therefore, the discovery of new drugs to combat resistant parasites is an urgent priority for malaria control.

Mollemycin A (MOMA), an azinothricin-type glyco-hexadepsipeptide-polyketide (Fig. 1), was discovered from an Australian marine-derived *Streptomyces* sp. (CMB-M0244) [3]. MOMA exhibits exceptionally potent growth-inhibitory activity against both drug-sensitive (3D7; $IC_{50}$ 7 nM) and multidrug-resistant (Dd2; $IC_{50}$ 9 nM) *Plasmodium falciparum* strains [3]. Its activity against resistant parasites and low cytotoxicity against mammalian cell lines [3] makes MOMA become a highly promising antimalarial candidate. However, the complexity of its chemical structure makes structural optimization through chemical approaches very challenging. So far, no successful strategies have been reported for the chemical synthesis or structural optimization of MOMA.

As an alternative to chemical synthesis, biosynthetic engineering proves to be an effective method for producing structural varieties of natural products, especially polyketides and non-ribosomal peptides which are assembled in a modular fashion [4–7]. However, the success of these approaches depends on the understanding of the biosynthetic mechanism and the achievement of a sufficient production titer of products, as engineering of biosynthetic genes usually reduces the yield. The endeavor of biosynthetic engineering is hindered by the limited understanding of the biosynthetic mechanism of MOMA and its low production yield in the wild-type strain. Therefore, we herein identified and characterized the biosynthetic pathway for MOMA. Furthermore, we improved the production of MOMA by optimizing the fermentation conditions and manipulating the two pivotal regulatory genes in the

Peer review under responsibility of KeAi Communications Co., Ltd.
* Corresponding author.
** Corresponding author. Australian Institute for Bioengineering and Nanotechnology, The University of Queensland, St Lucia, QLD, 4072, Australia.
*E-mail addresses:* x.jia@nus.edu.sg (X. Jia), chunlei@fudan.edu.cn (C. Lei).

https://doi.org/10.1016/j.synbio.2024.03.014
Received 19 January 2024; Received in revised form 27 February 2024; Accepted 19 March 2024
Available online 4 April 2024

MOMA biosynthetic pathway.

## 2. Materials and methods

### 2.1. Strains, plasmids, and culture conditions

The strain *Streptomyces* sp. (CMB-M0244) was kindly gifted by Robert Group at the University of Queensland (UQ), and other strains and plasmids used in this study are summarized in supplementary data (Table S1 and S2). *Escherichia coli* strains were cultured on Lysogeny Broth (LB) medium at 37 °C. The *Streptomyces* sp. (CMB-M0244) and its mutant strains were cultivated at 30 °C on a Mannitol Soybean powder (MS) agar medium or in a Tryptic Soy Broth (TSB) medium and fermented on M1-O agar medium at 30 °C for 7 days.

### 2.2. Genome sequencing and analysis

We extracted the genomic DNA (gDNA) of the MOMA-producing strain of *Streptomyces* sp. (CMB-M0244) using a method developed by Nikodinovic, Barrow and Chuck [8] with four minor modifications: 1) peptidase was not added, 2) lysozyme was increased to 5 mg $mL^{-1}$, 3) RNase was added to 20 μg $mL^{-1}$, and 4) the rotating step with chloroform was repeated if gDNA was contaminated by proteins. The final concentration of gDNA was 230 ng $\mu L^{-1}$ with an A260/A280 ratio of 1.77, confirming the negligible protein contamination in the gDNA sample.

After passing the quality control at the sequencing facility, genome sequencing was accomplished by Single Molecule Real-Time (SMRT) sequencing technology of Pacific Biosciences (PacBio) at UQ Centre for Clinical Genomics (UQCCG). Two SMRT cells were employed to generate 157,249 reads with a mean read length of 15,393 bp, which provided an average of × 193.49 coverage across the genome reference. The finished genome was assembled with HGAP2 [9].

Open reading frames were analyzed using the Frame Plot 4.0 beta online (http://nocardia.nih.go.jp/fp4/) and antibiotics and secondary metabolite analysis shell—antiSMASH [10], and the analysis of the deduced function of the proteins was carried out by the BLAST methods (http://blast.ncbi.nlm.nih.gov/Blast.cgi). Primer design, multiple nucleotide sequence alignments and analysis were performed using SnapGene.

### 2.3. General genetic manipulations and reagents

The general genetic manipulations in *E. coli* and *Streptomyces* were carried out following the standard protocols [11]. The primer synthesis and DNA sequencing were conducted at Tsingke Biotechnology Co., Ltd. Restriction endonuclease and DNA polymerase (Taq and Primestar) were purchased from Takara Biotechnology Co., Ltd. Primers are listed in Table S3. Unless otherwise specified, all chemical reagents were purchased from Shanghai Sangon Biotech Co., Ltd.

### 2.4. Construction of gene heterologous overexpression strains

For heterologous overexpression, a target gene was cloned into the vector pIB139, which contains an engineered constitutive promoter *kasOp** [12]. After sequencing confirmation, the recombinant plasmid was transformed into *E. coli* ET12567/pUZ8002 serving as the donor strain. Pre-processed *Streptomyces* as the recipient strain was mixed with the donor strain in proper proportion and spread onto MS agar medium added 10 mM $MgCl_2$ for conjugation. After 14 h, the mixture was overlaid with antibiotics apramycin (Am, 50 μg $mL^{-1}$) and trimethoprim (TMP, 50 μg $mL^{-1}$), then cultured at 30 °C for additional 3–5 days. Exconjugants, confirmed by polymerase chain reaction (PCR) with corresponding primers, were further cultivated for fermentation.

### 2.5. Construction of gene disruption strains

For gene disruption, a 1.5-kb DNA fragment from a target gene was inserted into the vector pYH7 [13]. After recombinant plasmid was transformed into *E. coli* ET12567/pUZ8002 cells and conjugated into *Streptomyces*, exconjugants were cultured in antibiotic-free TSB broth for 2–3 consecutive rounds to eliminate plasmids that had not integrated into the genome. Subsequently, the cultures were plated on MS agar medium with 50 μg $mL^{-1}$ Am to select strains integrated by the recombinant plasmid. The strains with correct gene disruptions, verified by PCR with two pairs of primers, were further cultivated for fermentation.

### 2.6. Construction of gene destruction strains

The vector pMWcas9 was used to inactive target gene clusters through destructing genes [14]. The spacer inserts, containing gene-specific 20 nucleotide guide sequences, were synthesized through the annealing of two 34 nucleotide oligonucleotides (Table S3), Sg1-sense/Sg1-antisense for *momB1* knock-out and Sg3-sense/Sg3-antisense for *momB3* knock-out in *Streptomyces* sp. (CMB-M0244). Subsequently, the annealed oligos were individually integrated into the pMWcas9 plasmid at the EcoRI-XbaI sites. Following this, two 1.8-kb homologous arms (left and right) for each gene were amplified from extracted genome DNA and seamlessly inserted into the

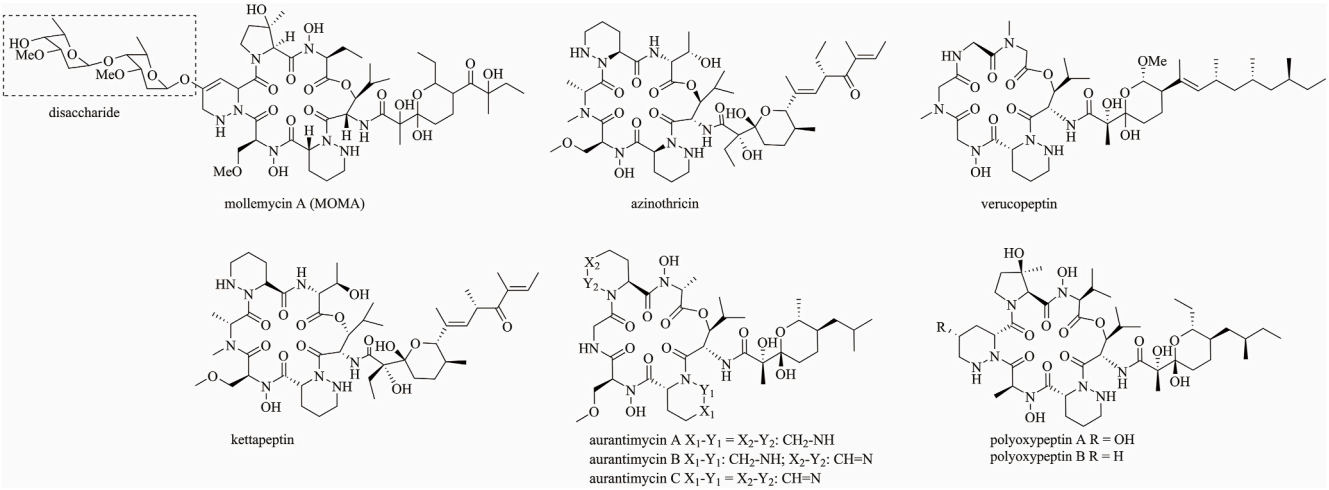


**Fig. 1.** Chemical structure of MOMA [3] whose disaccharide is highlighted by a dashed rectangle, and selected members of azinothricin family antibiotics.

aforementioned plasmids at HindIII site using infusion cloning kit, generating plasmid pFDU03B1 for *momB1* knock-out and plasmid pFDU03B3 for *momB3* knock-out. Following the transformation of the recombinant plasmid into *E. coli* ET12567/pUZ8002 cells and its subsequent conjugation into *Streptomyces*, apramycin-resistant exconjugants were cultured in 3 mL TSB medium containing 50 μg $mL^{-1}$ Am and 50 μg $mL^{-1}$ TMP, incubated at 30 °C for 2–3 days. Following this, 2 μg $mL^{-1}$ thiostrepton was introduced to induce the cleavage of the target DNA. The induced culture was then streaked onto an MS agar plate to isolate single colonies. To obtain plasmid-free progeny, colonies were streaked on a nonselective MS agar plate for 3–5 rounds and then it was plated on MS plates containing 5-fluorocytosine (200 μg $mL^{-1}$). The colonies capable of normal growth on these plates were identified as strains without plasmids. Each colony was inoculated into TSB liquid medium for mycelium growth, and gDNA was extracted and amplified by PCR using genotype confirmation primer pairs, VerB1F/VerB1R for *momB1* deletion and VerB3F/VerB3R for *momB3* deletion.

### 2.7. LC-MS analyses of fermentation products

After fermentation, the culture agar sliced into small pieces was soaked overnight in an equal volume of ethyl acetate and then extracted by ultrasonication. The extract, concentrated using a rotary evaporator under reduced pressure, was dissolved in chromatography-grade methanol and analyzed by UPLC-DAD-ESI (±) MS (Shimadzu LCMS-2020; Shim-pack GIST-HP C18, 2 μm, 2.1 × 50 mm). Buffer A is $H_2O$ with 0.1 % formic acid while buffer B is $CH_3CN$. The UPLC program runs at a flow rate of 0.2 mL $min^{-1}$ with the following gradient. The percentage of buffer B increased from 10 % at 0 min to 95 % at 10 min, remained at 95 % until 12 min and finally decreased back to 10 % at 13 min. The mass spectrometry program was in negative ion mode, with a scanning range of *m/z* 300-1800.

### 2.8. MOMA production evaluation

The fermentation agar of the wild-type strain on M1-O medium (5 L) was sliced into small pieces and subjected to ultrasonic extraction with an equal volume of ethyl acetate three times. This process generated a yellow crude extract (1.3 g), which was then suspended in $H_2O$ and further extracted successively with n-hexane, dichloromethane, ethyl acetate, and n-butanol. The dichloromethane fraction (0.4 g) underwent a column chromatography on Sephadex LH-20 (dichloromethane/methanol 1/1, v/v) to afford fractions A-F. Fraction B was subsequently purified by semi-preparative HPLC with a flow rate of 3.0 mL $min^{-1}$. MOMA was eluted at a retention time of 12.3 min, with a solvent composition of acetonitrile/water 45/55. The mass of MOMA was measured to be 6.5 mg. Therefore, the yield of MOMA in the wild-type strain was determined to be 1.3 mg $L^{-1}$. Given that MOMA peak area on extracted ion chromatograms is proportional to MOMA yield, the yield of MOMA in various mutants on M1-O medium was determined by integrating MOMA peak area on extracted ion chromatograms and comparing MOMA peak area between mutants and wild type.

### 2.9. Nucleotide sequence accession number

The sequence of mollemycin A biosynthetic gene cluster had been deposited in Genbank with an accession number of PP066841.

## 3. Results

### 3.1. Identification and analysis of mollemycin A biosynthetic gene cluster (*mom*)

Whole genome sequencing and assembling of *Streptomyces* sp. (CMB-M0244) generate two fragments with the size of 8,465,437 and 158,432 bases respectively, which indicates that the genome of this strain includes a standard linear chromosome and a large linear plasmid. Subsequently, we used web-based frame analysis to identify and annotate a gene cluster spanning 85.3 kilobase pairs, including 54 deduced open reading frames (ORFs). This cluster is hypothesized to be responsible for the biosynthesis of MOMA (Fig. 2a). Structural features of MOMA implicates that the biosynthesis of MOMA aglycone is synthesized by the hybrid polyketide synthases (PKSs)/non-ribosomal peptide synthetases (NRPSs). In accordance with the collinearity rule, each of four putative type I PKS genes (*momT*, *momU*, *momV* and *momW*) encodes one PKS module while four putative NRPS genes (*momX*, *momF*, *momG* and *momH*) collectively encode 6 NRPS modules. Besides, the gene *momZ1* is deduced to encode a glycosyltransferase and genes *momZ2-8* are associated with glycosyl synthesis. Additionally, three regulatory genes (*momB1*, *momB2* and *momB3*) have been identified, two of which (*momB1* and *momB3*) are LmbU-like and the other one (*momB2*) is homologous to the AfsR/SARP family transcriptional regulator (Table 1).

### 3.2. Verification of the MOMA biosynthetic gene cluster

After bioinformatics analysis of our postulated *mom* biosynthetic gene cluster (BGC), we validated it by disrupting the gene *momU*, which encodes one of the polyketide synthases. This disruption resulted in the abolishment of MOMA production.

The plasmid pFDU01U, generated by inserting a PCR-amplified 1.5 kb fragment from *momU* into vector pYH7, was introduced into the MOMA-producing strain and integrated into the genome by means of single crossover homologous recombination to construct a mutant MU01U (Fig. 2b). Confirmation of the pFDU01U integration into the chromosome was carried out via PCR using two pairs of specially designed primers: PverUF and PverpYR, PverpYF and PverUR. These primers included a forward primer with its corresponding primer complementary to either the *momU* gene or the vector pYH7. In the PCR amplification of the genomic DNA of wild-type strain, a band referring to the PCR amplified gene fragment of the theoretical size1.56 kb is observed, while it is absent in the mutant MU01U by using the primer pair (PverUF and PverUR). Conversely, no bands are observed in the PCR amplification of the wild-type strain's genome DNA whereas two bands corresponding to a theoretical size of 1.7 kb are present in mutant MU01U by using the primer pairs (PverUF and PverpYR; PverpYF and PverUR) (Fig. 2c). Taken together, the PCR product analyses conclude that the vector has been inserted into the genome of *Streptomyces* sp. (CMB-M0244). Subsequently, the LC-MS analysis of the fermentation agar of mutant MU01U shows that the production of MOMA is eradicated (Fig. 2d). Therefore, this deduced BGC accounts for MOMA biosynthesis.

### 3.3. Biosynthetic pathway of MOMA

We next propose a biosynthetic pathway of MOMA (Fig. 3), inspired by the deduced functions of all ORFs of *mom* gene cluster and referencing the biosynthetic pathway studies of vecucopeptin [15], aurantimycin [16], and polyoxypeptin [17] (those structures are shown in Fig. 1). As shown in Fig. 3b–h, a series of enzymes are assumed to be involved in catalyzing the syntheses of five building blocks for macrolide rings, including (*2S*,*3S*)-3-hydroxy-leucine, (*S*)–*N*-hydroxy-*α*-aminobutyric acid, (*S*)–*N*-hydroxy-serince, piperazic acid, 2-methylbutylmalonyl-CoA and (*2S*, *3R*)-3-hydroxy-3-methylproline. Besides modular NRPSs, seven free-standing NRPS genes in the *mom* gene cluster are deduced to individually encode two adenylation (A) domains (MomC and Mom6), two peptidyl carrier protein (T) domains (MomD and Mom7) and three thioesterase (TE) domains (MomS, MomI and MomY). Given that discrete NRPS domains in NRPS assembly lines regularly catalyze the formation of nonproteinogenic building blocks [18], MomC and Mom6 are proposed to activate leucine or (*2S*)-2-Methylbutyryl-CoA and subsequently tether them to MomD and

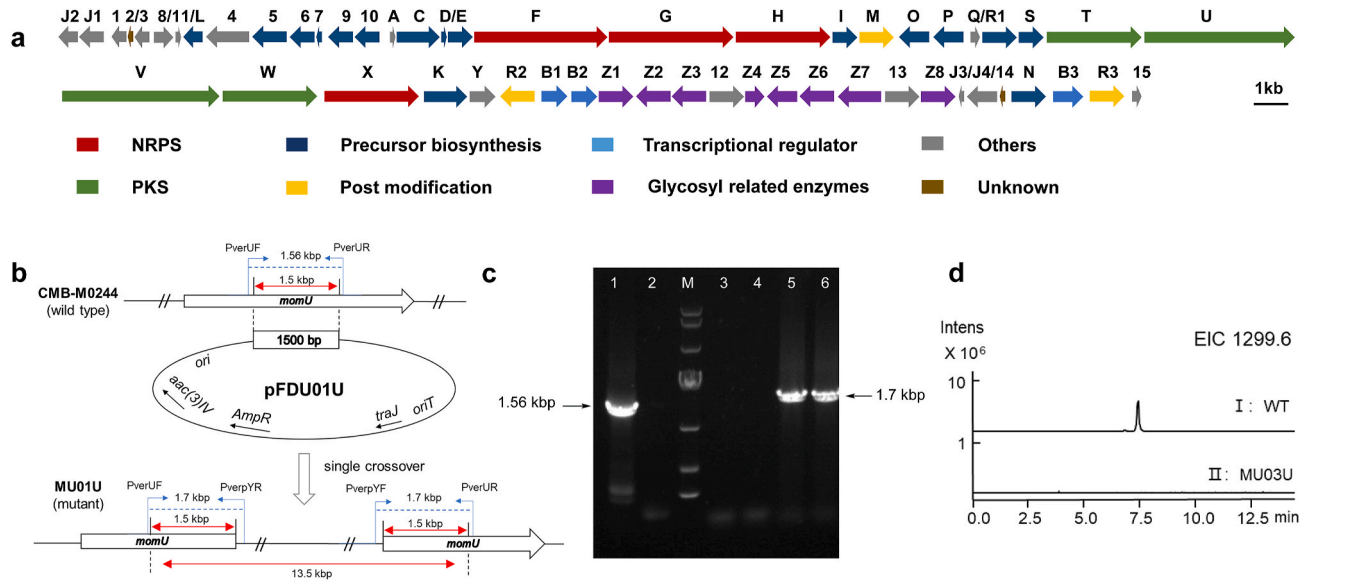


**Fig. 2.** Organization and confirmation of the *mom* biosynthetic gene cluster. a) Organization of the *mom* gene cluster. The proposed gene functions are listed in Table 1 b) Schematic construction of the *momU* disruption mutant MU01U. c) Confirmation of the *momU* disruption mutant MU01U by analyzing PCR products on an agarose gel electrophoresis. Lane 1, PCR product from a primer pair PverUF and PverUR with the wild type gDNA, Lane 3, PCR product from a primer pair PverUF and PverpYR with the wild type gDNA, Lane 4, PCR product with a primer pair PverpYF and PverUR with the wild type gDNA. Lanes 2, 5, and 6 are the same as lanes 1, 3, and 4 but with the mutant MU01U gDNA; M, 10 kb ladder. d) LC-MS analysis (extracted ion chromatograms of *m/z* $[M-H]^-$ 1299.6 corresponding to MOMA) of *Streptomyces* sp. (CMB-M0244) wild type (indicated with WT) and the mutant MU03U.

Mom7, respectively (Fig. 3b and e). The P450 enzyme MomR1 accounts for the installation of a hydroxyl group in 3-hydroxyleucine (Fig. 3b). MomK is predicted as L-lysine-6-monooxygenase and MomL is supposed to catalyze the formation of *N–N* bonds, potentially being responsible for the synthesis of piperazic acid [19–23] (Fig. 3f); The enzymes MomO, Mom5, and MomP are responsible for the synthesis of 3-hydroxy-3-methylproline (Fig. 3g); The enzymes Mom9, Mom10, Mom6, and MomI, along with a subset of primary metabolic enzymes, are inferred to synthesize a special extending unit 2-methylbutylmalonyl CoA (Fig. 3e).

Four PKSs (MomT, MomU, MomV and MomW), identified in *mom* biosynthetic gene cluster, share three foundational domains, i.e. ketosynthase domain (KS), acyltransferase domain (AT) and acyl-carrier protein (ACP), and contain exclusive domains. MomU carries a dehydratase (DH) and ketoreductase (KR) domain while MomV harbors a DH, enoylreductase (ER) and KR domain. The loading or extending unit selected by AT can be predicted through "fingerprint residue" of AT [24]. Generally, GHS(I/Q)G and HAFH motifs represent AT specific to malonyl-CoA while GHSQG and YASH represent AT specific to (*2S*)-methylmalonyl-CoA (Fig. S1). GHSQG and YASH motifs in AT of MomT indicate that MomT-AT recognizes methylmalonyl-CoA and loads a propionate acyl onto ACP. KS domain of MomT, however, is inactive because in the active site motif "SGQ" does a glutamine residue substitute for a cysteine residue so that transthioesterification reaction cannot occur (Fig. S2). Therefore, MomT is an initiating PKS module for methylmalonyl-CoA. AT of the following extending PKS MomU, special with unique motifs VPGH which may broaden the substrate binding pocket and enhance its hydrophobicity than HAFH and YASH (Fig. S1), likely takes an unusual and bulky extending unit 2-methylbutylmalonyl-CoA. Following a similar principle, the extending unit of PKS MomV is malonyl-CoA and that of MomW is (*2S*)-methylmalonyl-CoA. The DH domain in MomU is speculated to be inactive because the key acid residue histidine is replaced by arginine in the conserved motif HxxxGxxxxP [25,26] (Fig. S3), which is consistent with the retention of a hydroxyl group. The presence of LDD motifs and the absence of proline at two downstream positions of catalytic tyrosine indicate that both the KR domains of MomU and MomV belong to the B1-type KRs [27], suggesting the presence of a hydroxyl group with an *R*-configuration (Fig. S4).

After the PKS chain is synthesized, MomX catalyzes the formation of an amide bond. The chain is then transferred to 3-hydroxyleucine, whose hydroxyl group plays a key role in subsequent cyclization, triggering the assembly of peptide core structure. MomF contains two modules with eight domains (C-A1-T-E-C-A2-MT-T), while MomG contains two modules with seven domains (C-A1-T-E-C-A2-T). Both MomF-A1 and MomG-A1 are proposed to recognize and activate L-piperazic acid based on the conserved substrate specificity-conferring amino acids (DVFSVAGYAK for MomF-A1, DVFSVAAYAK for MomG-A1) (Fig. S5), which are highly analogous to those of KtzH-A1 (DVFSVGPYAK) [20] and PlyG-A1 (DVFSIAAYAK) [17]. The epimerization (E) domain then converts the L-piperazine acid block to D-configuration on the assembly line. In MomF, the methyltransferase (MT) domain catalyzes *O*-methylation in the L-Serine residue recognized by MomF-A2. MomG-A2, with motifs DVFCNSSYAK, likely recognizes and activates 3-hydroxyl-3-methyl-proline.

Once these biosynthetic building blocks are sequentially condensed, the TE domain in MomH catalyzes release of the chain from the peptidyl carrier protein via hydrolysis, accompanied by cyclization through ester bond formation to generate the 19-membered macrocyclic intermediate MOM-Int1. Subsequently, this intermediate undergoes further hydroxylation in multiple steps facilitated by the P450 enzymes MomM, MomR2 and MomR3, ultimately leading to MOMA aglycone (Fig. 3a). Finally, the glycosyltransferase MomZ1 sequentially transfers two molecules of oleander-*O*-TDP (Fig. 3h), synthesized by MomZ2-MomZ8 cluster, to the aglycone, completing the biosynthesis of MOMA.

### 3.4. *MomB2 is the positive regulator and MomB3 is the negative regulator during MOMA biosynthesis*

Within the *mom* gene cluster, three putative regulatory genes *momB1*, *momB2* and *momB3* are believed to regulate the production of MOMA. To understand their functions, we employ a combination of genetic manipulation of these regulatory genes and resultant MOMA production analysis due to these genetic manipulations.

Firstly, plasmids are constructed to overexpress each regulatory

**Table 1**
Deduced functions of ORFs in the biosynthetic gene cluster of MOMA.

| Proteins | Amino acids | Proposed function | Homologous protein species | Accession no. | Identity/Similarity |
|---|---|---|---|---|---|
| MomJ2 | 260 | ABC transporter permease | *Streptomyces janthinus* | WP_193482711 | 89%/96% |
| MomJ1 | 333 | Daunorubicin/doxorubicin resistance ABC transporter | *Streptomyces davaonensis* JCM 4913 | CCK31805 | 85%/90% |
| Mom1 | 145 | DUF2089 domain-containing protein | *Streptomyces antimycoticus* | WP_137964791 | 78%/88% |
| Mom2 | 86 | hypothetical protein | *Streptomyces atriruber* | WP_055567845 | 73%/80% |
| Mom3 | 133 | DUF2089 family protein | *Streptomyces* sp. DSM 44918 | WP_311595120 | 81%/90% |
| Mom8 | 254 | DUF1707 domain-containing protein | *Streptomyces janthinus* | WP_193477330 | 72%/79% |
| Mom11 | 74 | ferredoxin | *Streptomyces janthinus* | WP_230529232 | 79%/87% |
| MomL | 220 | FMN-binding negative transcriptional regulator | *Streptomyces janthinus* | WP_193477331 | 78%/87% |
| Mom4 | 505 | FAD-dependent monooxygenase | *Streptomyces janthinus* | WP_193477332 | 86%/91% |
| Mom5 | 414 | zinc-binding dehydrogenase | *Streptomyces phaeofaciens* | WP_229870298 | 87%/92% |
| Mom6 | 312 | ketoacyl-ACP synthase III | *Actinacidiphila yanglinensis* | WP_103883639 | 82%/89% |
| Mom7 | 82 | ACP | *Streptomyces* sp. GC420 | WP_166628105 | 83%/93% |
| Mom9 | 326 | 2-oxoisovalerate dehydrogenase subunit beta | *Embleya hyalina* | WP_246126487 | 86%/92% |
| Mom10 | 308 | 3-methyl-2-oxobutanoate dehydrogenase subunit alpha | *Streptomyces* sp. AVP053U2 | ODA73935 | 79%/87% |
| MomA | 71 | MbtH family protein | *Streptomyces* sp. NWU339 | WP_109379533 | 87%/95% |
| MomC | 519 | amino acid adenylation domain-containing protein | *Streptomyces janthinus* | WP_193477339 | 80%/86% |
| MomD | 84 | phosphopantetheine-binding protein | *Streptomyces* sp. NWU339 | PWI09282 | 83%/92% |
| MomE | 395 | NAD(P)/FAD-dependent oxidoreductase | *Streptomyces phaeochromogenes* | WP_073491942 | 85%/92% |
| MomF | 2872 | NRPS (C-A-T-E-C-A-MT-T) | *Streptomyces fodineus* | WP_069778199 | 82%/88% |
| MomG | 2593 | NRPS (C-A-T-E-C-A-T) | *Streptomyces* sp. NRRL S-920 | WP_030795270 | 79%/86% |
| MomH | 1254 | NRPS (C-A-T-TE) | *Streptomyces fodineus* | AOR31553 | 82%/88% |
| MomI | 245 | thioesterase | *Streptomyces aureoverticillatus* | GGS26058 | 78%/86% |
| MomM | 427 | cytochrome P450 | *Streptomyces* sp. NRRL S-920 | WP_051819881 | 78%/87% |
| MomO | 308 | phytanoyl-CoA dioxygenase family protein | *Streptomyces* sp. NRRL S-920 | WP_030788363 | 88%/93% |
| MomP | 270 | l-proline 3-hydroxylase type II | *Streptomyces* sp. MK498-98F14 | AGZ15468 | 74%/84% |
| MomQ | 103 | ACP | *Streptomyces* sp. NRRL S-920 | WP_030788369 | 74%/85% |
| MomR1 | 413 | cytochrome P450 | *Streptomyces* sp. NRRL S-920 | WP_030788371 | 87%/92% |
| MomS | 245 | thioesterase domain-containing protein | *Streptomyces janthinus* | WP_193477350 | 79%/85% |
| MomT | 1019 | type I PKS (KS-AT-T) | *Streptomyces cellostaticus* | WP_079057806 | 75%/82% |
| MomU | 1852 | type I PKS (KS-AT-DH-KR-T) | *Streptomyces janthinus* | WP_230529237 | 76%/82% |
| MomV | 2199 | type I PKS (KS-AT-DH-ER-KR-T) | *Streptomyces janthinus* | WP_193477351 | 76%/83% |
| MomW | 1032 | type I PKS (KS-AT-T) | *Streptomyces janthinus* | WP_193477352 | 83%/89% |
| MomX | 1057 | NRPS (C-A-T) | *Streptomyces* sp. NWU339 | PWI09293 | 72%/81% |
| MomK | 458 | l-lysine 6-monooxygenase | *Streptomyces phaeoluteigriseus* | OQD55129 | 81%/87% |
| MomY | 248 | thioesterase | *Streptomyces noursei* | GGX52622 | 74%/82% |
| MomR2 | 389 | cytochrome P450 | *Streptomyces janthinus* | WP_193477359 | 86%/93% |
| MomB1 | 258 | LmbU family transcriptional regulator | *Streptomyces janthinus* | WP_193477372 | 69%/79% |
| MomB2 | 254 | AfsR/SARP family transcriptional regulator | *Streptomyces* sp. CWNU-1 | WP_250920819 | 87%/93% |
| MomZ1 | 435 | glycosyl transferase | *Streptomyces janthinus* | WP_230529241 | 72%/83% |
| MomZ2 | 327 | dTDP-glucose 4,6-dehydratase | *Streptomyces* sp. NRRL S-920 | WP_030788407 | 88%/93% |
| MomZ3 | 302 | glucose-1-phosphate thymidylyltransferase RfbA | *Streptomyces* sp. NRRL S-920 | WP_030788410 | 86%/92% |
| Mom12 | 381 | transposase | *Streptomyces fodineus* | WP_079161262 | 76%/85% |
| MomZ4 | 198 | dTDP-4-dehydrorhamnose 3,5-epimerase family protein | *Streptomyces fodineus* | WP_069778181 | 78%/83% |
| MomZ5 | 259 | dTDP-6-deoxy-l-hexose 3-O-methyltransferase | *Streptomyces* | WP_015506844 | 71%/83% |
| MomZ6 | 336 | aldo/keto reductase | *Streptomyces fodineus* | WP_069778176 | 90%/95% |
| MomZ7 | 478 | NDP-hexose 2,3-dehydratase family protein | *Streptomyces* sp. BA2 | WP_160501911 | 74%/81% |
| Mom13 | 385 | 3′,5′-cyclic AMP phosphodiesterase CpdA | *Streptomyces* sp. yr375 | SEQ18001 | 54%/65% |
| MomZ8 | 307 | NAD-dependent epimerase/dehydratase | *Streptomyces* sp. NRRL S-920 | WP_250920830 | 75%/83% |
| MomJ3 | 63 | ABC transporter permease | *Arthrobacter alpinus* | WP_062006921 | 61%/75% |
| MomJ4 | 274 | ATP-binding cassette domain-containing protein | *Streptosporangium amethystogenes* | WP_030904273 | 75%/84% |
| Mom14 | 86 | hypothetical protein | *Streptomyces janthinus* | WP_193477369 | 72%/75% |
| MomN | 426 | valine–pyruvate transaminase | *Streptomyces janthinus* | WP_310849879 | 81%/87% |
| MomB3 | 286 | LmbU family transcriptional regulator | *Streptomyces janthinus* | WP_193477372 | 71%/79% |
| MomR3 | 401 | cytochrome P450 | *Streptomyces janthinus* | WP_193477373 | 88%/95% |
| Mom15 | 120 | ISL3 family transposase | *Streptomyces* sp. 378 | WP_283974958 | 89%/91% |

gene: pFDU02B1 for *momB1* (Fig. S6), pFDU02B2 for *momB2* (Fig. S7) and pFDU02B3 for *momB3* (Fig. S8). These gene overexpression plasmids were individually conjugated into *Streptomyces* sp. (CMB-M0244) to generate mutant strains: MU02B1 for *momB1* overexpression, MU02B2 for *momB2* overexpression and MU02B3 for *momB3* overexpression (Fig. S6-8). The fermentation samples of the mutants and wild type strain were analyzed by LC-MS to quantify MOMA production (Fig. 4). The results show that the MOMA production by MU02B2 mutant increases to about 150 % (Fig. 4, trace IV), and that by MU02B1 (Fig. 4a, trace II) and MU02B3 (Fig. 4a, trace V) mutants are significantly reduced to almost nil, which suggesting MomB2 acts as a positive regulator while MomB1 and MomB3 act as negative regulators. To validate this conclusion, two new inactivating mutants (MU03B1 and MU03B3) were created. In MU03B1, *momB1* was in-frame deleted using plasmid pFDU03B1 (Fig. S9), while in MU03B3, *momB3* was in-frame deleted using plasmid pFDU03B3 (Fig. S10). Fermentation analysis of these two mutants reveals that the MU03B3 mutant shows a 250% increase in MOMA production (Fig. 4a, trace VI), solidifying its negative regulatory role. Surprisingly, the MU03B1 mutant completely lacks MOMA production (Fig. 4a, trace III). This unexpected outcome requires further investigation to determine the true function of MomB1. Finally, we created a synergic mutant where *momB3* was deleted while *momB2* was overexpressed. This synergic mutant further boosts the yield of MOMA to 2.6 times higher than the wild-type strain (Fig. 4a, trace VII and Fig. 4b).

### 3.5. Optimization of fermentation conditions and utilization of genetic engineering boost MOMA production

Using the yield of MOMA as the evaluation standard, M1, the

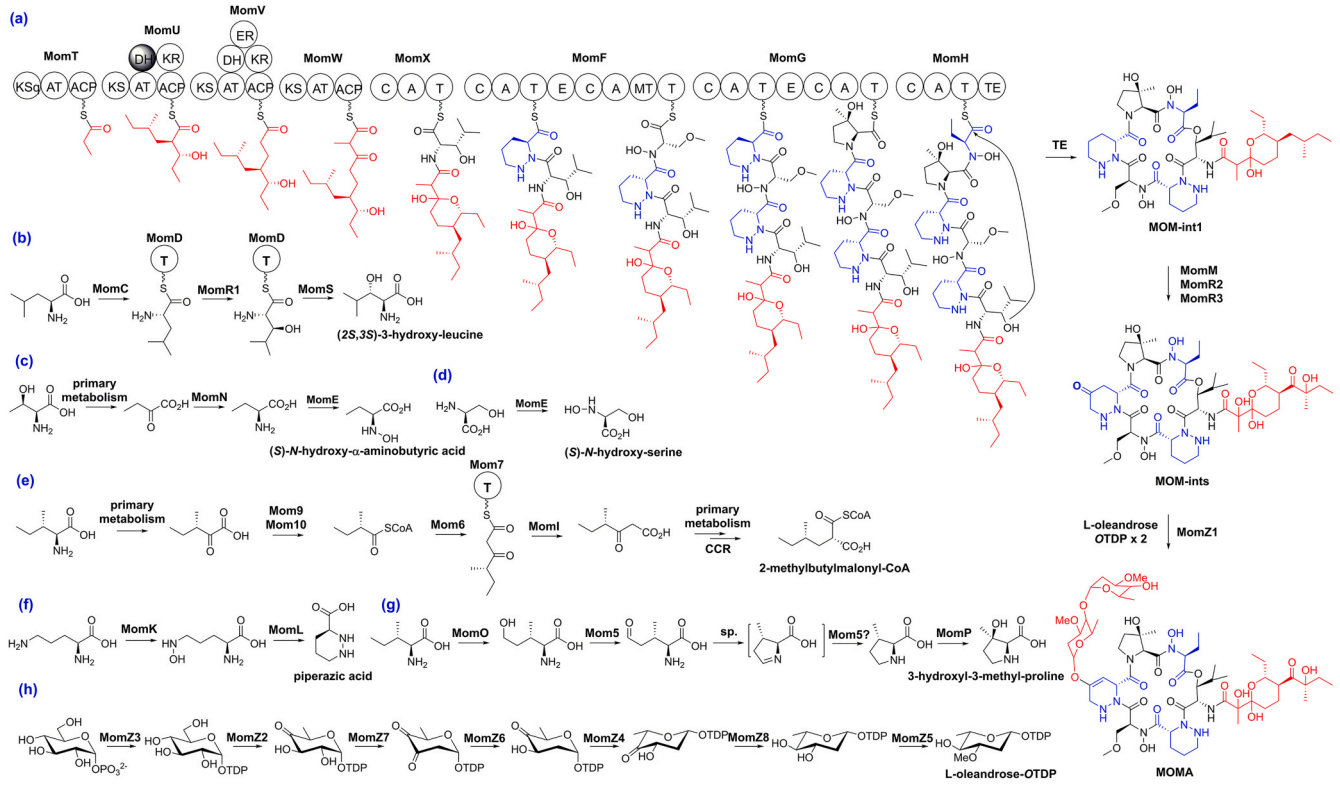


**Fig. 3.** Proposed biosynthetic pathway for MOMA. a) The proposed biosynthetic pathway for MOM scaffold assembly line driven by the hybrid PKS/NRPS system. KS stands for ketosynthase, AT for acyltransferase, ACP for acyl carrier protein, DH for dehydratase, KR for ketoreductase, ER for enoylreductase, A for adenylation domain, T for peptidyl carrier protein, C for condensation domain, MT for methyltransferase domain, E for epimerase domain and TE for thioesterase domain. b-h) The proposed pathways for the biosynthesis of building blocks.

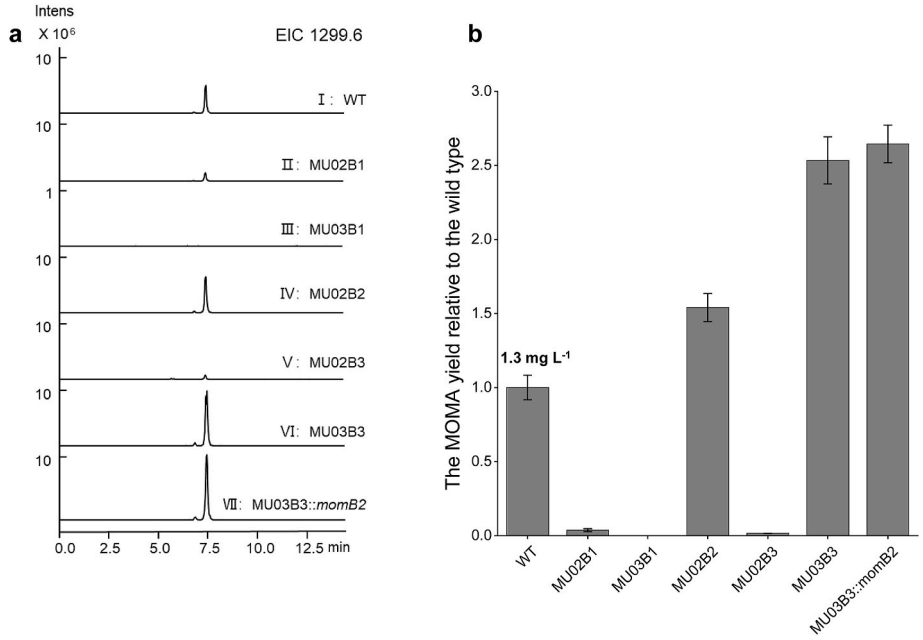


**Fig. 4.** Genetic characterization of *momB1*, *B2* and *B3*. The role of *momB2* is determined as a positive regulatory and *momB3* as a negative regulatory gene for MOMA biosynthesis. a) LC-MS analysis (extracted ion chromatograms of *m/z* [M − H]$^-$ 1299.6 corresponding to MOMA) of *Streptomyces* sp. (CMB-M0244) wild type (indicated with WT) and mutants (MU02B1, MU03B1, MU02B2, MU02B3, and MU03B3). b) Relative yield of MOMA production in various mutant strains compared to the wild type (WT), which is 1.3 mg L$^{-1}$. The yield was determined by analyzing the integrated peak area of extracted ion chromatograms corresponding to MOMA, where MOMA peak area in the wild type is normalized to 1. The synergic strain MU03B3::*momB2* has the highest yield of MOMA, nearly 2.6 fold increase times greater than the wild type. The replication number is three.

medium reported in the literature [3], was found to have a better fermentation effect than other commonly used *Streptomyces* fermentation media like MS and ISP-2 in the laboratory. In production, the performance of M1 on agar medium format was significantly better than that in its broth format. Single-factor experiments targeting fermentation time showed that the optimal fermentation time is 7 days. Subsequently, an orthogonal experiment with four factors (sea salt, soluble starch, peptone and yeast exact) and three levels (high, middle and low) was designed to optimize the ratio of each component in M1 agar medium (Table S4 and S5). The experimental results are shown in Table S5. The experimental range (R value) analysis reveals that the influence of various factors on the production of MOMA follows a descending order of soluble starch, yeast extract, peptone and sea salt. As sea salt has the least impact, it is used as an error variation for variance analysis (Table S6). Among them, the *p*value of soluble starch is less than 0.05, indicating a significant impact on the yield of MOMA. Therefore, the optimal medium, named M1-O, is composed of 33 g sea salt, 5 g soluble starch, 2 g peptone and 4 g yeast extract per liter, which increased yield by approximately 50 % from 0.9 mg $L^{-1}$ to 1.3 mg $L^{-1}$.

In summary, our study achieves a remarkable two-pronged enhancement of MOMA production. Firstly, we optimize the fermentation medium by formulating M1-O, which boosts MOMA yield from 0.9 mg $L^{-1}$ to 1.3 mg $L^{-1}$ by an impressive 50 %. Secondly, we engineered a synergistic mutant strain by deleting the *momB3* gene and overexpressing *momB2*, resulting in a 2.6-fold increase from 1.3 mg $L^{-1}$ to 3.4 mg $L^{-1}$. These findings pave the way for the development of highly efficient strains for the sustainable and economical production of MOMA and its analogues.

## 4. Discussion

Varying degrees of resistance have been emerged to all known antimalarial drugs, making the discovery and research of novel antimalarial compounds imperative and urgent [1]. MOMA, with its promising *in vitro* antimalarial activity, is worthy of further research to diversify its structures and potentially achieve enhanced activity and reduced toxicity. Therefore, this study has unraveled, and characterized the biosynthetic gene cluster of MOMA for the first time, speculated on its complex biosynthetic pathway and identified strategies to increase MOMA production.

PKSs typically utilize acyl-CoA thioesters from the pool of primary metabolites, such as acetyl-CoA, malonyl-CoA, and methylmalonyl-CoA, as two- or three-carbon building blocks for chain assembly [28]. Notably, MOMA biosynthetic pathway employs an unusual seven-carbon extension unit, 2-methylbutylmalonyl CoA, captured by the AT domain in MomU. This suggests broader substrate recognition capabilities for MomU-AT compared to conventional PKS AT domains. Sequence alignments revealed functional similarity between MomU-AT and ArtP-AT, the AT domain involved in aurantimycin biosynthesis [16]. Both ATs possess the conserved VPGH motif whereas ArtP-AT recognizes 2-(2-methylpropyl) malonyl-CoA as an extender unit. This opens the possibility of feeding 4-methylpentanoic acid or other structurally similar small molecule carboxylic acids during fermentation, which could be converted to their corresponding acyl-CoA forms with the assistance of AntE [29] or Arm13-associated acyl-CoA carboxylase [30] that are integrated into the genome, to generate novel MOMA analogues.

Interestingly, MOMA is the only reported azinothricin family member with a disaccharide chain composed of two L-oleandrose units. Glycosylation is often associated with enhanced bioactivity in various antibiotics [31], including arimetamycin A [32], thiazomycins [33], vancomycin [34], and avermectin [35]. L-oleandrose specifically has been identified as a key active group in the antiparasitic activity of avermectin [36,37]. Elucidating the mechanism of L-oleandrose transfer to the MOMA core skeleton could pave the way for modifying and broadening the biological activities of azinothricin family.

Low MOMA production in *Streptomyces* sp. (CMB-M0244) poses a challenge for downstream analysis, including structural analogues isolation, separation, and preparation of substrates for enzyme activity assay. Consequently, to increase the production of MOMA, we implemented combined strategies of fermentation optimization and genetic engineering, resulting in a great increase in MOMA production. This improvement effectively facilitates future research and contributes to the development of high-yielding industrial strains.

In conclusion, the identification and characterization of *mom* gene cluster, along with the enhanced MOMA production, lays a solid foundation for a deeper understanding of its biosynthetic pathway and mechanisms. This study empowers the design and creation of novel MOMA-based antibiotics with improved antimalarial activity and modified selectivity through synthetic biology approaches.

## CRediT authorship contribution statement

**Shixue Jin:** Methodology, Investigation, Formal analysis, Visualization, Writing – original draft. **Huixue Chen:** Investigation, Formal analysis. **Jun Zhang:** Formal analysis, Visualization. **Zhi Lin:** Methodology. **Xudong Qu:** Conceptualization, Funding acquisition, Resources. **Xinying Jia:** Investigation, Funding acquisition, Visualization, Writing – review & editing. **Chun Lei:** Conceptualization, Project administration, Supervision, Resources, Writing – review & editing.

## Declaration of generative AI and AI-assisted technologies in the writing process

During the preparation of this work the authors used ChatGPT 3.5 in order to improve the language. After using this tool, the authors reviewed and edited the content as needed and take full responsibility for the content of the publication.

## Declaration of competing interest

The authors declare that they have no known competing financial interests or personal relationships that could have appeared to influence the work reported in this paper.

## Acknowledgement

This work was financially supported by The University of Queensland (UQ postdoctoral fellowship to X. Jia) and the National Natural Science Foundation of China (no. 31970054 to X. Qu). We thank Mr. Lawrie Wheeler at The University of Queensland Centre for Clinical Genomics for his PacBio sequencing of the genome of mollemycin A producing strain. We also appreciate Dr. Zeinab G. Khalil at Institute for Molecular Bioscience, The University of Queensland, for her assistant in the strain transfer and her preparation of mycelium samples for genomic DNA extraction.

## Appendix A. Supplementary data

Supplementary data to this article can be found online at https://doi.org/10.1016/j.synbio.2024.03.014.

## References

[1] World malaria report 2023. Geneva: World Health Organization; 2023. Licence: CC BY-NC-SA 3.0 IGO.
[2] World Health Organization. Global technical strategy for malaria 2016-2030. 2021. https://iris.who.int/handle/10665/342995. update [accessed 31 December 2023].
[3] Raju R, Khalil ZG, Piggott AM, Blumenthal A, Gardiner DL, Skinner-Adams TS, et al. Mollemycin A: an antimalarial and antibacterial glyco-hexadepsipeptide-polyketide from an Australian marine-derived *Streptomyces* sp. (CMB-M0244). Org Lett 2014;16(6):1716–9. https://doi.org/10.1021/ol5003913.

[4] Katsuyama Y, Miyanaga A. Recent advances in the structural biology of modular polyketide synthases and nonribosomal peptide synthetases. Curr Opin Chem Biol 2022;71:102223. https://doi.org/10.1016/j.cbpa.2022.102223.
[5] Winn M, Fyans JK, Zhuo Y, Micklefield J. Recent advances in engineering nonribosomal peptide assembly lines. Nat Prod Rep 2016;33(2):317–47. https://doi.org/10.1039/c5np00099h.
[6] Du L, Sanchez C, Shen B. Hybrid peptide-polyketide natural products: biosynthesis and prospects toward engineering novel molecules. Metab Eng 2001;3(1):78–95. https://doi.org/10.1006/mben.2000.0171.
[7] Beck C, Garzón JFG, Weber T. Recent advances in Re-engineering modular PKS and NRPS assembly lines. Biotechnol Bioproc Eng 2020;25(6):886–94. https://doi.org/10.1007/s12257-020-0265-5.
[8] Nikodinovic J, Barrow KD, Chuck JA. High yield preparation of genomic DNA from *Streptomyces*. Biotechniques 2003;35(5):932. https://doi.org/10.2144/03355bm05.
[9] Chin CS, Alexander DH, Marks P, Klammer AA, Drake J, Heiner C, et al. Nonhybrid, finished microbial genome assemblies from long-read SMRT sequencing data. Nat Methods 2013;10(6):563–9. https://doi.org/10.1038/nmeth.2474.
[10] Blin K, Shaw S, Steinke K, Villebro R, Ziemert N, Lee SY, et al. antiSMASH 5.0: updates to the secondary metabolite genome mining pipeline. Nucleic Acids Res 2019;47(W1):W81. https://doi.org/10.1093/nar/gkz310. w7.
[11] Green MR, Sambrook J. Molecular cloning: a Laboratory Manual. fourth ed. New York: COLD SPRING HARBOR LABORATORY PRESS; 2012.
[12] Wang W, Li X, Wang J, Xiang S, Feng X, Yang K. An engineered strong promoter for *streptomycetes*. Appl Environ Microbiol 2013;79(14):4484–92. https://doi.org/10.1128/aem.00985-13.
[13] Sun Y, Hong H, Samborskyy M, Mironenko T, Leadlay PF, Haydock SF. Organization of the biosynthetic gene cluster in *Streptomyces* sp. DSM 4137 for the novel neuroprotectant polyketide meridamycin. Microbiology (Read) 2006;152(Pt 12):3507–15. https://doi.org/10.1099/mic.0.29176-0.
[14] Mo J, Wang S, Zhang W, Li C, Deng Z, Zhang L, et al. Efficient editing DNA regions with high sequence identity in actinomycetal genomes by a CRISPR-Cas9 system. Synth Syst Biotechnol 2019;4(2):86–91. https://doi.org/10.1016/j.synbio.2019.02.004.
[15] Zhang L, Wang Y, Huang W, Wei Y, Jiang Z, Kong L, et al. Biosynthesis and chemical Diversification of verucopeptin leads to structural and functional versatility. Org Lett 2020;22(11):4366–71. https://doi.org/10.1021/acs.orglett.0c01387.
[16] Zhao H, Wang L, Wan D, Qi J, Gong R, Deng Z, et al. Characterization of the aurantimycin biosynthetic gene cluster and enhancing its production by manipulating two pathway-specific activators in *Streptomyces aurantiacus* JA 4570. Microb Cell Factories 2016;15(1):160. https://doi.org/10.1186/s12934-016-0559-7.
[17] Du Y, Wang Y, Huang T, Tao M, Deng Z, Lin S. Identification and characterization of the biosynthetic gene cluster of polyoxypeptin A, a potent apoptosis inducer. BMC Microbiol 2014;1430. https://doi.org/10.1186/1471-2180-14-30.
[18] Fischbach MA, Walsh CT. Assembly-line enzymology for polyketide and nonribosomal Peptide antibiotics: logic, machinery, and mechanisms. Chem Rev 2006;106(8):3468–96. https://doi.org/10.1021/cr0503097.
[19] Du Y, He H, Higgins MA, Ryan KS. A heme-dependent enzyme forms the nitrogen-nitrogen bond in piperazate. Nat Chem Biol 2017;13(8):836–8. https://doi.org/10.1038/nchembio.2411.
[20] Wei ZW, Niikura H, Morgan KD, Vacariu CM, Andersen RJ, Ryan KS. Free piperazic acid as a precursor to nonribosomal peptides. J Am Chem Soc 2022;144(30):13556–64. https://doi.org/10.1021/jacs.2c03660.
[21] Morgan KD, Andersen RJ, Ryan KS. Piperazic acid-containing natural products: structures and biosynthesis. Nat Prod Rep 2019;36(12):1628–53. https://doi.org/10.1039/c8np00076j.
[22] Stephan P, Langley C, Winkler D, Basquin J, Caputi L, O'Connor SE, et al. Directed evolution of piperazic acid incorporation by a nonribosomal peptide synthetase. Angew Chem Int Ed Engl 2023;62(35):e202304843. https://doi.org/10.1002/anie.202304843.
[23] Shin D, Byun WS, Kang S, Kang I, Bae ES, An JS, et al. Targeted and logical discovery of piperazic acid-bearing natural products based on genomic and spectroscopic signatures. J Am Chem Soc 2023;145(36):19676–90. https://doi.org/10.1021/jacs.3c04699.
[24] Yadav G, Gokhale RS, Mohanty D. Computational approach for prediction of domain organization and substrate specificity of modular polyketide synthases. J Mol Biol 2003;328(2):335–63. https://doi.org/10.1016/s0022-2836(03)00232-8.
[25] Moriguchi T, Kezuka Y, Nonaka T, Ebizuka Y, Fujii I. Hidden function of catalytic domain in 6-methylsalicylic acid synthase for product release. J Biol Chem 2010;285(20):15637–43. https://doi.org/10.1074/jbc.M110.107391.
[26] Moriguchi T, Ebizuka Y, Fujii I. Domain-domain interactions in the iterative type I polyketide synthase ATX from *Aspergillus terreus*. Chembiochem 2008;9(8):1207–12. https://doi.org/10.1002/cbic.200700691.
[27] Zheng J. 1.03 - structural biology of tailoring domains in polyketide synthases. In: Liu H, Begley T, editors. Comprehensive natural products III. Oxford: Elsevier; 2020. p. 47–60.
[28] Liou GF, Khosla C. Building-block selectivity of polyketide synthases. Curr Opin Chem Biol 2003;7(2):279–84. https://doi.org/10.1016/s1367-5931(03)00016-4.
[29] Yan Y, Zhang L, Ito T, Qu X, Asakawa Y, Awakawa T, et al. Biosynthetic pathway for high structural diversity of a common dilactone core in antimycin production. Org Lett 2012;14(16):4142–5. https://doi.org/10.1021/ol301785x.
[30] Zhang J, Zheng M, Yan J, Deng Z, Zhu D, Qu X. A permissive medium chain acyl-CoA carboxylase enables the efficient biosynthesis of extender units for engineering polyketide carbon scaffolds. ACS Catal 2021;11(19):12179–85. https://doi.org/10.1021/acscatal.1c03818.
[31] Kren V, Rezanka T. Sweet antibiotics - the role of glycosidic residues in antibiotic and antitumor activity and their randomization. FEMS Microbiol Rev 2008;32(5):858–89. https://doi.org/10.1111/j.1574-6976.2008.00124.x.
[32] Kang HS, Brady SF. Arimetamycin A: improving clinically relevant families of natural products through sequence-guided screening of soil metagenomes. Angew Chem Int Ed 2013;52(42):11063–7. https://doi.org/10.1002/anie.201305109.
[33] Zhang C, Herath K, Jayasuriya H, Ondeyka JG, Zink DL, Occi J, et al. Thiazomycins, thiazolyl peptide antibiotics from *Amycolatopsis fastidiosa*. J Nat Prod 2009;72(5):841–7. https://doi.org/10.1021/np800783b.
[34] Yim G, Thaker MN, Koteva K, Wright G. Glycopeptide antibiotic biosynthesis. J Antibiot (Tokyo) 2014;67(1):31–41. https://doi.org/10.1038/ja.2013.117.
[35] Ikeda H, Nonomiya T, Usami M, Ohta T, Omura S. Organization of the biosynthetic gene cluster for the polyketide anthelmintic macrolide avermectin in *Streptomyces avermitilis*. Proc Natl Acad Sci U S A 1999;96(17):9509–14. https://doi.org/10.1073/pnas.96.17.9509.
[36] Chabala JC, Mrozik H, Tolman RL, Eskola P, Lusi A, Peterson LH, et al. Ivermectin, a new broad-spectrum antiparasitic agent. J Med Chem 1980;23(10):1134–6. https://doi.org/10.1021/jm00184a014.
[37] Dong L, Zhang J. Research progress of avermectin: a minireview based on the structural derivatization of avermectin. Advanced Agrochem 2022;1(2):100–12. https://doi.org/10.1016/j.aac.2022.11.001.